Base Dependent DNA-carbon Nanotube Interactions: Activation Enthalpies and Assembly-disassembly Control

Base dependent DNA-carbon nanotube interactions: activation enthalpies and assembly-disassembly control

Running head: Base dependent DNA-carbon nanotube interactions

Fernando Albertorio[1], Mary E. Hughes[2], Jene A. Golovchenko[1,2] and Daniel Branton[3]*

1. Department of Physics, Harvard University, Cambridge, MA 02138
2. School of Engineering & Applied Sciences, Harvard University, Cambridge, MA 02138
3. Department of Molecular & Cellular Biology, Harvard University, Cambridge MA 02138

*Corresponding author. Contact information:

Department of Molecular & Cellular Biology, Harvard University

16 Divinity Avenue

Cambridge, MA 02138

Telephone: 617-495-2685

E-mail: dbranton@harvard.edu

We quantify the base dependent interactions between single stranded DNA and single walled carbon nanotubes (SWNT) in solution. DNA/SWNT hybrids hold the promise of applications ranging from nanoscale electronics and assembly of nanotube based materials, to drug delivery and DNA sequencing. These applications require control over the hybrid assembly and disassembly. Our analytical assay reveals the order of nucleobase binding strengths with SWNTs as G > C > A > T. Furthermore, time dependent fixed temperature experiments that probe the kinetics of the dissociation process provide values for the equilibrium constants and dissociation enthalpies that underlie the microscopic interactions. Quantifying the base dependency of hybrid stability shows how insight into the energetics of the component interactions facilitates control over hybrid assembly and disassembly.

1. Introduction

Single stranded DNA (ssDNA) and single walled carbon nanotubes (SWNT) interact in solution, under sonication, to form a charged hybrid structure, DNA/SWNT[1,2]. The aromatic nucleobases are believed to π-stack with the nanotube's graphene side walls[1,3-5]. By acting as a scaffold, single walled nanotubes confine and orient DNA molecules, thus opening the door to many applications in nano- and biotechnology[6-10]. We have reported that each of the four nucleobases (Guanine, Cytosine, Adenine, and Thymine) orient in distinct ways with respect to the nanotube's long axis[3]. Both AFM images and spectroscopic studies of DNA/SWNTs have suggested that the DNA spontaneously wraps itself around nanotubes[2,11-13]. But absent evidence that all of the bases in a DNA molecule are associated with the nanotube's surface, one must consider the possibility that not all of the DNA bases are π-stacked with the nanotube's graphene side walls or that DNA may not always assume a simple helical conformation around the nanotube[14-16].

Synthetic single stranded oligonucleotides (homopolymers or simple sequences typically of lengths <100 bases) have been widely used in forming DNA/SWNTs. It has been reported that various ssDNA polymers of alternating sequences facilitate the separation of nanotubes by electronic property[1,2,17]. This suggests that the nanotube's electronic state and the base composition of the DNA

determine the properties of the resulting DNA-nanotube hybrid[4,5,18-20]. To date, the influence of individual nucleobases over the molecular interaction between DNA and a SWNT remains to be quantified.

Many applications involving DNA/SWNT will require controlling both the assembly and disassembly of the hybrid. For example, if DNA is used to sort nanotubes by diameter, chirality, or electronic behavior, the DNA must ultimately be removed to recover clean, sorted nanotubes[11,21-23]. This is especially critical if the nanotubes are to be assembled into electronic devices. Furthermore, the effectiveness of DNA/SWNT hybrids as vehicles for gene or drug delivery[7,8,10,24,25] hinges on the nanotubes' ability to release their cargo within the cell. Thus, understanding the binding and unbinding of the DNA bases with SWNTs, along with the factors that contribute to the stability of the ensemble, will be important in choosing the correct base composition, length, and solution conditions for the many potential applications of these hybrids.

A few experimental measurements have been made to characterize the factors that determine the association and dissociation of DNA to SWNTs. Some half-life times for flocculation of DNA/SWNT held at 90^{o}C were reported[26], as were the base dependent efficiencies of different DNAs to disperse nanotubes during ultrasonication[1,27]. Not only are these results qualitative because the environment that the DNA and nanotubes experience during sonication cannot be precisely duplicated, but we suspected that dispersability trends may not necessarily correlate with quantitative measures of binding strength. Complementary base-pairing between ssDNA in solution and ssDNA bound to a nanotube[28,29] has been examined, but a simple direct assay of DNA-SWNT hybrid stability and its dependence on the specific nucleobases of the DNA is still lacking.

We present a rapid analytical method to quantify the association and dissociation of ssDNA to single walled nanotubes. By probing the specific base dissociation temperatures of homo-oligonucleotide/SWNT hybrids, the thermodynamics of processes that govern the stability of DNA/SWNT in solution is elucidated. Furthermore, we demonstrate control over the hybrid assembly

and disassembly by tuning specific solution conditions such as ionic strength and free DNA concentration.

2. Experimental section

2.1. Preparation of hybrids

A 1 mg/ml solution of twelve base-long single stranded DNA homopolymers consisting of poly $d(A)_{12}$, poly $d(T)_{12}$, poly $d(C)_{12}$ or poly $d(G)_{12}$ (reverse-phase purification grade, Midland Certified Reagent Company, Midland, Texas and henceforth sometimes referred to as A, T, C, or G, respectively) in phosphate buffered saline (PBS buffer: 50mM sodium phosphate, 100mM sodium chloride, pH 7.5) was added to HiPCO single walled carbon nanotubes (Carbon Nanotechnologies, Houston, Texas) at a 1:1 DNA:SWNT mass ratio. The HiPCO SWNTs consist of both semiconducting and metallic tubes of various chiralities with diameters ranging from 0.8 - 1.2 nm[25]. The DNA/SWNT mixture was surrounded by an ice bath and sonicated (Vibra Cell probe VCX130PB, Sonics and Materials Inc., Newton, CT) at a power of ~5 W for 30 min. As previously described [3], centrifugation (16,000g at 4^{o}C for 30 min.) removed bundles of non-dispersed nanotubes and size-exclusion chromatography (using Micro Bio-Spin P-30 columns, Bio-Rad, Hercules, California) removed any remaining free DNA. After size exclusion chromatography we determined that the amount of free DNA (as described below) in the supernatant was less than 30 ng/ml. Prior to any assay, the DNA/SWNT dispersions were maintained at 4^{o}C to prevent dissociation of the DNA from the nanotubes.

We chose twelve base long oligomers for all of our assays because short single stranded DNA sequences (<5 bases) do not provide a good yield of hybrids whereas long DNA oligos (>20 bases) create hybrids that are difficult to thermally dissociate over reasonably short assay periods. We found that 12 base-long oligomers provided a high yield of hybrids yet dissociated within sufficiently short times to also provide a very reproducible, convenient, short assay. PBS buffer was used for all the experiments because sodium phosphate has a buffering stability over our working temperature range ($\Delta pH/\Delta T$ = -0.003 pH-units/^{o}C)[30].

2.2. Isochronal temperature assay

This assay (figure 1, Incubation variable: temperature) quantifies the hybrid's thermal stability. It does so by indirectly measuring the extent to which 12 base long ssDNA polymers dissociate from nanotubes after incubation in an aqueous buffer solution at different temperatures (4^0 – 99^0 C) for a fixed amount of time (chosen for convenience as 10 minutes).

The initial DNA/SWNT dispersion was separated into multiple 100 μL aliquots in thin-walled PCR tubes. Each tube was held at the desired temperature (4 - 99°C) for 10 minutes using a home-built linear temperature gradient device. As DNA dissociated from the SWNT, the bare nanotubes re-bundled in solution forming aggregates (herein referred to as $SWNT_{aggregate}$). Afterwards, the samples were cooled on ice to quench any further dissociation of DNA from the nanotubes. A critical step in our assay scheme was the removal of the $SWNT_{aggregate}$ by centrifugation (16,000g at 4°C for 30 min) to assure that light scattering did not interfere with the accuracy of our optical absorption measurements. The supernatant containing the remaining dispersed DNA/SWNT hybrids was collected and its optical absorption at 815 nm was determined (Shimadzu UV-260). We determined the fraction of dispersed hybrids, defined as α[*DNA/SWNT*], by dividing the absorbance of the DNA/SWNT that remained suspended after centrifugation by that of the initial hybrid dispersion, $DNA/SWNT_{initial}$. $DNA/SWNT_{initial}$ was the 4°C control sample in which no DNA dissociation was observed (i.e. absolute OD value remained constant). The incubation temperature at which 50% of the hybrids remained in solution after the 10 minute incubation was defined as $T_{1/2}$. Our detection wavelength at 815 nm corresponds to a Van Hove singularity in semiconducting SWNT[31] which constitute 75% of the HiPCO prepration. Although control experiments that probed other wavelength peaks in the range of 400-900nm did not show significantly different $T_{1/2}$ values (within ±1°C, data not shown), the conveniently quick assay presented here may not reveal subtle but important differences in DNA's organization and binding strength on different types of carbon nanotubes.

2.3. Assaying free DNA

To confirm that the isochronal temperature assay indeed measured DNA dissociation from the nanotubes, we determined the concentration of free ssDNA released to the incubation solution during the assay described above. We modified a standard method for precipitating double stranded DNA[32] so as to first separate the hybrids from the free ssDNA in solution. Although the mechanism of charge screening induced by the addition of ethanol in the presence of DNA/SWNTs is unknown, it appeared that the addition of alcohol screened the stabilizing electrostatic force between the DNA coated nanotubes, causing them to fall out of solution. We initially characterized the precipitation method to determine the amount of ethanol needed to achieve effective precipitation of hybrids without precipitating free ssDNA in solution. A 10:1 ethanol:PBS buffer provided the most effective separation. Therefore, a 10:1 (ethanol:buffer) solution at 4^0C was added to each of the samples containing DNA/SWNT that were to be assayed for free DNA. After centrifugation at 16,000g at 4^oC for 3 minutes, the precipitated DNA/SWNT in each sample formed a tight pellet at the bottom of the eppendorf tube and the supernatant containing unbound DNA was collected. Next, we performed control experiments to characterize the efficiency of the 10:1 ratio (ethanol:buffer) in precipitating the free ssDNA. Compared to the 2:1 alcohol:water ratio usually used to precipitate DNA, the 10:1 ratio is an inefficient method of precipitating ssDNA, particularly short ssDNA oligos (in our case 12mers). Nevertheless, to avoid dilution and loss of material, we optimized the incubation time and temperature and, after having found that an overnight incubation at 4^oC in 10:1 alcohol:water recovered 85 +/- 10% of free the ssDNA in a control solution containing no nanotubes (data not shown), we used such overnight incubations at 4^oC to precipitate the free ssDNA in our samples. After centrifugation (16,000g at 4^oC for 30 min), the pelleted DNA was rehydrated to its original volume with PBS buffer and the ssDNA concentration was determined by UV absorption at 260nm. Performing this extraction on a freshly prepared DNA/SWNT sample yielded no detectable DNA, confirming that the procedure itself did not remove any DNA from the nanotubes.

2.4. Langmuir isotherm

We found that the addition of free DNA to an existing DNA/SWNT dispersion suppressed dissociation of the DNA from the nanotubes at all temperatures. This allowed us to determine the dissociation equilibrium constant K_d for $d(T)_{12}$/SWNT hybrid at 25 ^oC. A solution of $d(T)_{12}$/SWNT was separated into multiple 75 μL aliquots. An amount of $d(T)_{12}$ ssDNA in 25 μL of PBS was added to each sample to achieve the desired final free DNA concentration in the range from 0μM to 300μM (figure 1, Incubation Variable: free DNA). The 0μM sample received PBS containing no DNA. After a 480 hour equilibration period, the samples were centrifuged and the supernatants were optically probed as in the isochronal temperature assays, above. The extent to which DNA/SWNT dissociation was suppressed by the addition of free DNA was determined by dividing the absorbance of the DNA/SWNT that remained suspended after centrifugation by that of the initial DNA/SWNT, as in the isochronal temperature assays, above.

2.5. Kinetics and Eyring analysis

To study the energetics of DNA molecular interaction with SWNT, we first obtained the dissociation rate constants (k_{off}) by monitoring the change in the concentration of dispersed DNA/SWNT hybrids as a function of time (figure 1, Incubation Variable: time). By probing the kinetics as a function of temperature, we extracted the activation enthalpies of hybrid dissociation. Experimentally, the initial DNA/SWNT dispersion was separated into 100 μL aliquots, and each aliquot was heated to one of four temperatures, 60^{o}C, 70^{o}C, 80^{o}C, or 90^{o}C. At each chosen time point, a tube was removed and treated in the same manner as in the isochronal temperature assay, that is, cooled, centrifuged and the supernatant optically probed. We determined the fraction of dispersed hybrids $\alpha[DNA/SWNT]$ as in the isochronal temperature assay described above, except that in this case the $DNA/SWNT_{initial}$ was the 'zero time' reference sample.

3. Results and Discussion

3.1. Thermo-stability of DNA/SWNT hybrid.

The isochronal temperature assay presented here measures the stability of DNA binding to SWNT in solution at different temperatures. When the dispersed hybrids are exposed to different temperatures (range 4 - 99 ^{o}C), DNA dissociates from the hybrid, and the exposed nanotubes aggregate or bundle in solution via van der Waals and hydrophobic interactions [33]. These aggregates are easily sedimented before determining the optical absorption of the clear supernatant at 815 nm, a wavelength at which the nanotubes absorb light, but DNA does not (figure 1). The temperature dependent fraction remaining in solution is fit to a sigmoidal function (figure 2), from which we extract $T_{1/2}$, the temperature at which 50% of the hybrids remain in solution.

The measurements obtained for the twelve-base ssDNA/SWNT hybrids show that $T_{1/2}$ is a characteristic property of the particular oligo/SWNT being tested and reveal that the hybrid stability of homopolymers to nanotubes varies as G > C > A~T (figure 2). These results differ from the hybrid stabilities derived from two recent molecular dynamic simulation studies which predict that G>A>T>C[34] or T>(GT)>G[35]. The reasons for these differing orders of hybrid stabilities could be related to differences in the particular starting assumptions or experimental conditions, differences in type and geometry of nanotubes assumed, or to higher order, base-dependent effects that may not currently taken into account in molecular dynamic studies. The availability of the quantitative but rapid and simple assay described here should make it possible to provide experimentally verifiable hybrid stabilities with different starting and experimental conditions, and different nanotube types and geometries (when purified samples of just one nanotube type and geometry become available).

We confirmed that as the fraction of suspended nanotubes decreases, the amount of free DNA increases (figure 2, inset). The quaternary hydrogen-bonded structures which can form between neighboring guanine homopolymers[36] may contribute to the markedly greater thermo-stability of poly $d(G)_{12}$/SWNT ($T_{1/2}$ >100^{o} C) compared to $d(C)_{12}$/SWNT, $d(A)_{12}$/SWNT, and $d(T)_{12}$/SWNT. We considered several other factors that may affect the stability of DNA/SWNTs in solution, but found no

correlation between stability and the nucleotides' dipole moments[37], polarizability[38], hydrophobicity[39], structure[40], or size[41]. Our experimentally determined absence of correlation differs from computational studies that predict that the total π-stacking energy associated with the van der Waals attraction during hybrid self-assembly correlate with the nucleobase surface area, i.e. stronger binding for purines (A and G) than for pyrimidines (C and T)[34].

We further demonstrate that the hybrid dissociation temperature $T_{1/2}$ may be determined by the way in which particular polynucleotides interact with themselves when associating with a nanotube. For example, we observe that the thermo-stability of poly $d(GT)_6$/SWNT ($T_{1/2}$ = 85 ^oC) is greater than that of the poly $d(AC)_6$/SWNT hybrids ($T_{1/2}$ = 61 ^oC) (figure 3). These results show that the stability is not a simple average of the $T_{1/2}$ values for each of the two constituent bases in each heteropolymer. It is tempting to interpret our results with $d(GT)_6$ and $d(AC)_6$ as support for the hypothesis that non Watson-Crick base pairing of $d(GT)_6$ with itself via H-bonding accounts for its greater stability than the poly $d(AC)_6$, which is not known to form such bonds[2,42]. But since molecular dynamics simulations show that the dimerization of poly d(GT) is energetically unfavorable[34], it may well be that other currently unknown factors account for the different $T_{1/2}$ values between poly $d(GT)_6$ and poly $d(AC)_6$. Nevertheless, our results with heteropolymers show that sequence complexity, which does introduce the possibility of H-bonding between complementary bases, may alter hybrid stability. Furthermore, our ability to differentiate between hybrids containing oligonucleotides that can or cannot form non-Watson-Crick hydrogen bonding between themselves suggests that nanotubes could be used to probe and concentrate specific base-enriched DNA sequences.

The role of DNA's ionized phosphate backbone in stabilizing the hybrid should also be considered. The sugar-phosphate backbone interacts with the aqueous environment and prevents the hybrid from aggregating, thus causing hybrids to behave like a colloid in solution. Molecular dynamic simulations suggest that the sugar-phosphate backbone determines how the DNA spontaneously rearranges on the tube surface[34]. The ionic strength dependence of hybrid stability is evident in that the $T_{1/2}$ of $d(C)_{12}$/SWNT is shifted ~70^oC downward as the NaCl concentration is increased from 100 mM to

1,000 mM and conversely, DNA/SWNT dissociation is suppressed when the supporting electrolyte concentration is reduced to 0 mM (not shown). Again, this demonstrates our ability to selectively tune how readily DNA dissociates from nantubes under various aqueous conditions as needed for applications involving these hybrids.

$T_{1/2}$ is not a true equilibrium parameter; rather, it is a simple 'snap-shot' of the hybrid dissociation kinetics at an arbitrarily selected time. While the absolute values of $T_{1/2}$ will depend on the assay incubation time, our kinetic experiments below show that the relative stability of the interaction between particular polynucleotides and nanotubes is maintained even after many hours of incubation. Furthermore, given that HiPCO SWNTs are a collection of tubes that have different chiralities, electronic properties, lengths and diameters, and because high yields of one particular nanotube type are not readily available today, the value of $T_{1/2}$ represents an average value of DNA's binding stability to many different kinds of nanotubes. We speculate that, were it possible to achieve high yields of nanotubes of a given type (i.e., diameter, electrical properties, etc.), the differences between the several DNA/SWNT stabilities observed here with different nucleobases may be similar or even greater. For instance, replica exchange molecular dynamics simulation was used to study the thermal stability of 10-mer homo-oligos of d(T), d(GT) and d(G) interacting with nanotubes of particular chirality[35]. As the temperature increases, the number of π-stacking interaction between the bases of a single DNA molecule and the tube decreases, revealing a particular order in nucleobase stability as d(T) > d(GT) > d(G)[35]. Our, control experiments (data not shown) using COMOCAT SWNTs consisting of a diameter distribution between 1.2 - 1.5 nm showed statistically similar $T_{1/2}$ when compared with HiPCO SWNTs whose diameters ranged from 0.8 nm – 1.2 nm).

3.2. Hybrid dissociation kinetics and equilibrium

To quantify the dynamics of hybrid stability, we probed the time dependence of the DNA dissociation from nanotubes at a fixed temperature. Figure 4a shows the dissociation kinetics of $d(T)_{12}$/SWNTs at

room temperature starting with hybrids dispersed in solution devoid of free DNA. The observed unbinding process is:

$$DNA/SWNT \rightarrow DNA_{free} + SWNT_{aggregate} \quad (1)$$

where DNA/SWNT represents the nanotubes with associated DNA that remain suspended, and $SWNT_{aggregate}$ are nanotubes that have lost sufficient DNA so that they aggregate and precipitate, thus making the process irreversible. The data can be fit by an exponential decay of the following form:

$$\alpha(t) = ce^{-k_{off}t} + d \quad (2)$$

where α is the fraction of the initial DNA/SWNT hybrids that remain suspended at time t, k_{off} (which was found to be = 1/59 h^{-1}) is the rate constant for the observed first order process, and d = 0.22 is the fraction of the initial DNA/SWNT that remained suspended even after 160h. The non-zero value of d suggests that steady-state equilibrium is established between the DNA/SWNTs that had lost some of their DNA and free DNA, which reached a concentration of ~0.8 μM at 160 hours.

To test whether reaction (1) could reach a steady state equilibrium in the presence of free DNA, we added known amounts of poly $d(T)_{12}$ (0 - 300 μM) to freshly prepared $d(T)_{12}$/SWNT (initially devoid of free DNA). We determined the fraction of DNA/SWNT that remained in solution as a function of added DNA after 20 days at room temperature (25 ^{o}C). In the presence of greater than 50 μM added free DNA, nanotube aggregation and the consequent irreversible dissociation of the hybrid were clearly suppressed (figure 4b). Thus, in the presence of free DNA in solution, reaction (1) is reversible and reaches a steady state equilibrium expressed as:

$$DNA/SWNT \rightleftharpoons DNA_{free} + SWNT_{depleted} \quad (3)$$

where $SWNT_{depleted}$ are nanotubes that have lost a fraction of their DNA, but still retain sufficient DNA to remain in solution. Since we are probing the total fraction of remaining DNA/SWNT hybrids in solution, it is not necessary to know what fraction of DNA is lost *per single nanotube* to generate irreversible aggregation. The $SWNT_{aggregate}$ term is not present in (3) since these aggregated nanotubes are removed by centrifugation.

To extract what we will call an effective equilibrium dissociation constant, K_d, from figure 4b, we consider the following:

$$K_d = \frac{[SWNT_{depleted}][DNA_{free}]}{[DNA/SWNT]} \tag{4}$$

Rearranging equation (4) to become

$$[SWNT_{depleted}] = \frac{[DNA/SWNT]K_d}{[DNA_{free}]} \tag{4.1}$$

the equilibrium fraction of remaining hybrids as a function of added free DNA that we measure as *t* approaches infinity can be written:

$$\alpha(t \to \infty) = \frac{[DNA/SWNT]}{[DNA/SWNT_{initial}]} = \frac{[DNA/SWNT]}{[DNA/SWNT]+[SWNT_{depleted}]} \tag{4.2}$$

Substituting the expression for $[SWNT_{depleted}]$ from equation (4.1) into equation (4.2), we find:

$$\alpha(t \to \infty) = \frac{[DNA_{free}]}{K_d + [DNA_{free}]} \tag{5}$$

This equation describes a Langmuir isotherm[43] where K_d is the concentration of free DNA at which 50% of the hybrids remain in solution. For the case of poly $d(T)_{12}$/SWNT hybrids, we obtain an effective K_d of 11.2 +/- 3.1 μM.

We call the observed K_d an 'effective' dissociation constant because the Hill-Langmuir equation (5) requires that the fraction of dispersed DNA/SWNT equal zero at zero concentration of free DNA. Our system is unable to satisfy this requirement. We approach the condition of zero free DNA concentration immediately after size-exclusion chromatography, but during experimental incubation, the sample recovered from size-exclusion chromatography becomes a dispersion of SWNTs containing a variable amount of DNA per unit length of nanotube. Thus, the concentration of DNA we report is not the sum of free + bound DNA concentration in the sample, but the free DNA concentration in excess of the amount of DNA that initially associated with the SWNTs. Furthermore, one typically defines the equilibrium dissociation constant taken from equation 5 as the concentration at which 50% of the molecules are in the

complexed form. In our system, we define K_d as the DNA concentration in which 50% of the hybrids remain in solution. Our sample consists of more than just "unformed" and "formed" species; that is, the stoichiometry of DNA to nanotube that maintains SWNT solubility is unknown and it is very likely that a nanotube remains in solution even after losing some of its initially hybridized DNA. Because the concentration of free DNA we report is the amount of free ssDNA added to the hybrids in solution, we cannot estimate the concentration of DNA *on* the nanotubes. We note that these approximations to the Langmuir model in measuring K_d make estimates of ΔG unreliable. Nevertheless, our value of the "effective K_d" is a first approach to the equilibrium between ssDNA and SWNTs. The importance of knowing this equilibrium process will be evident for applications requiring the long-term stability of DNA/SWNT solutions and for drug or gene delivery.

A consequence of DNA rebinding to SWNTs is that the $T_{1/2}$ of $d(T)_{12}$/SWNT increases from 71.9°C to ~ 90°C when 140 μM free DNA is added to the purified DNA/SWNT preparation (figure 5). This finding has implications for applications where the shelf-life of the hybrid is important. Hybrids formed with short oligos (≤12 bases) will, even at room temperature, dissociate and lead to irreversible nanotube aggregation in the absence of ca. ≥ 140 μM free DNA in the suspension. Our finding means that the typically short shelf-life of such hybrids (a few hours) can be increased over extended periods of time and ranges of temperatures by adding free DNA.

Equations 4 and 5 imply that the sonication process used to assemble hybrids is required only to disaggregate the initially bundled tubes, allowing DNA to gain access to the thus exposed SWNT. This means that short oligonucleotides, used for the initial suspension of nanotubes by sonication, should be replaceable with longer ssDNA by simple incubation, without requiring the sonication that would normally shear such kilobase-length polymers. Slow equilibrium processes have also been observed with double stranded DNA (dsDNA), which required up to ~35 days to fully cover the nanotube surface[44].

3.3. Energetics of hybrid disassembly

The temperature dependence on the rate of hybrid dissociation determines the activation enthalpies of dissociation. As an example, figure 6a presents dissociation rate curves for T = 99°C, 80°C, 70°C, and

60°C for $d(A)_{12}$/SWNT. We compared the dissociation rates taken at 99°C for each of the DNA/SWNT hybrids. Although we have not evaluated the order of the dissociation rate expression (reaction 1), we found that the rate curves fit best to a single exponential (equation 2), suggesting that our data is best described using a first order kinetic model. The values of k_{off} and τ (τ is the half-time for the first order dissociation process obtained from equation 2 reveal the same order in nucleobase binding strength d(G) > d(C) > d(A) > d(T). The kinetic studies allow us to resolve differences in binding strengths between polymers of A and T, which were otherwise undistinguishable using the isochronal temperature assay.

To extract the activation enthalpies of dissociation, the temperature dependent rate constants (figure 6b) are inserted in the Eyring[45] equation

$$\ln\left(\frac{k_{off}(T)}{T}\right) = -\frac{\Delta H}{RT} + \frac{\Delta S}{R} + \ln\left(\frac{\kappa R}{N_A h}\right) \qquad (6)$$

where k_{off} is the observed rate constant, ΔH is the activation enthalpy, ΔS is the activation entropy, N_A is Avogadro's number, κ is the transmission coefficient (usually set to 1), and *h* Planck's constant, enables determination of the activation enthalpies (table 1). Once again, in applying equation (6) to the reaction of equation (1), we make the simplifying assumption that our experiments are performed on hybrids that have an average number of DNA molecules/unit length of SWNT such that incremental fractional loss of DNA leads to incremental nanotube aggregation.

Our activation dissociation enthalpies of DNA/SWNTs quantitatively confirm the strong dependence of the hybrids' stabilities on the specific polynucleotide, d(C) > d(A) > d(T). (Poly d(G) was not studied because of difficulties in reliably achieving the yields needed for this experiment.) The trend of the results (table 1) agrees with the observed order of $T_{1/2}$ obtained from the isochronal temperature assay. Because the temperature dependence of the dissociation rate constants could only be acquired for a narrow range of temperatures (60 – 99°C), we cannot report useful values for the entropy because of the huge uncertainty that would be introduced in attempting to extrapolate from our data towards the very distant 'y' intercept which determines the ΔS value. The activation energy of salmon testes dsDNA molecules binding to nanotubes was recently determined to be in the range of 7.4 - 9.8 kcal/mole[44].

But our hybrid stability measurements are difficult to correlate with these important observations using dsDNA where the initial binding interaction may be complicated by factors other than nucleobase π-stacking to the nanotube sidewalls; hydrogen bonds between complementary bases of dsDNA are known to compete with the DNA-SWNT interaction and remove DNA from nanotube surfaces[33].

In principle, one can determine the rate of DNA binding to SWNTs, k_{on}, from $k_{on} = k_{of}/K_d$, from which we calculate $k_{on} = 0.33\ M^{-1}s^{-1}$. A diffusion limited rate constant[43] would be $\sim 10^{10}\ M^{-1}s^{-1}$, a value much higher than our observed k_{on}. We conclude that a barrier must be overcome before DNA can bind to the nanotube. The energy landscape may be even more complicated where entropy gain or loss may contribute to the energy cost that comes from ssDNA bases unstacking and reorganization onto the nanotube's graphene sidewalls. It has been shown that rearrangement of high molecular weight dsDNA takes place on the nanotube's surface during long timescales of a few months, leading to a more ordered structure[44]. It will be of interest in the future to experimentally determine whether the hybrid association barrier is primarily entropic or enthalpic.

4. Conclusion

Our analytical assay represents a first step in experimentally quantifying the strength of the interaction between ssDNA and single walled carbon nanotubes. The isochronal dissociation temperature ($T_{1/2}$) is a property of the type of oligonucleotide interacting with the nanotubes. The nucleobase dependence of hybrid stability (G > C > A > T) quantified by our measurements of the dissociation enthalpy suggests that the hydrophobic π-stacking that is suggested to be the main driving force for hybrid self-assembly[34,35,46], is not the only contributor to DNA's interaction with the curved graphitic surfaces of the nanotube. Other factors, such as the electrostatic interaction between the phosphate backbone and the aqueous environment, base stacking within the single stranded polymer, and geometric and stereochemical limitations, may account for why our results are not identical to experimentally observed trends for ssDNA interaction with flat graphitic surfaces, where the order of nucleobase binding strengths was found to be G > A > T > C[47,48]. DNA conformational strain may be very different for a

given polynucleotide that is constrained on a flat graphitic surface *versus* a very small diameter curved surface.

Future applications of our method to determine the activation dissociation enthalpy may provide insight into the molecular organization of DNA on carbon nanotubes. If we assume that all the nucleobases are π-stacked with the SWNT walls, then dividing the value of ΔH by the number of constituent bases (here, N = 12, table 1) will yield the enthalpy contribution per nucleobase. If all the nucleobases are π-stacked with the SWNT walls, the value of ΔH/base will be independent of the polymer length and our estimated dissociation enthalpies per nucleobase would range from 1.2 to 2.0 kcal/mole (2.1 k_BT to 3.5 k_BT). These values are within the range of the enthalpy of nucleoside base stacking as measured by a dangling-end thermo-denaturation assay (-2 to 4.5 kcal/mole)[49]. On the other hand, if *not all* of the nucleobases are π-stacking on the nanotube sidewall[14-16], then the measured ΔH will not vary linearly with the oligonucleotide's length. Future studies based on the methodology presented here will make it possible to determine which of these assumptions is correct and should complement single molecule studies aimed at resolving the physical interactions that take place between a DNA molecule and a SWNT.

Acknowledgments. Support for this research has been provided by National Institutes of Health #R01HG003703 and Ruth L. Kirschstein National Research Service Award #1F32HG004692 to F. Albertorio.

References

[1] Zheng M, Jagota A, Semke E D, Diner B A, McLean R S, Lustig S R, Richardson R E and Tassi N G 2003 DNA-assisted dispersion and separation of carbon nanotubes *Nature Materials* **2** 338-42

[2] Zheng M, Jagota A, Strano M S, Santos A P, Barone P, Chou S G, Diner B A, Dresselhaus M S, McLean R S, Onoa G B, Samsonidze G G, Semke E D, Usrey M and Walls D J 2003 Structure-based carbon nanotube sorting by sequence-dependent DNA assembly *Science* **302** 1545-8

[3] Hughes M E, Brandin E and Golovchenko J A 2007 Optical absorption of DNA-carbon nanotube structures *Nano Lett.* **7** 1191-4

[4] Meng S, Maragakis P, Papaloukas C and Kaxiras E 2007 DNA nucleoside interaction and identification with carbon nanotubes *Nano Lett.* **7** 45-50

[5] Meng S, Wang W L, Maragakis P and Kaxiras E 2007 Determination of DNA-base orientation on carbon nanotubes through directional optical absorbance *Nano Lett.* **7** 2312-6

[6] Lu Y, Bangsaruntip S, Wang X, Zhang L, Nishi Y and Dai H 2006 DNA-functionalization of carbon nanotubes for ultra-thin atomic layer deposition of high K dielectrics for nanotube transistors with 60 mV/decade switching *J. Am. Chem. Soc.* **128** 3518-9

[7] Barone P W, Baik S, Heller D A and Strano M S 2005 Near-infrared optical sensors based on single-walled carbon nanotubes *Nature Materials* **4** 86-92

[8] Feazell R P, Nakayama-Ratchford N, Dai H and Lippard S J 2007 Soluble single-walled carbon nanotubes as longboat delivery systems for platinum(IV) anticancer drug design *J. Am. Chem. Soc.* **129** 8438-9

[9] Kam N W, O'Connell M J, Wisdom J A and Dai H 2005 Carbon nanotubes as multifunctional biological transporters and near-infrared agents for selective cancer cell destruction *Proc. Natl. Acad. Sci. U.S.A.* **102** 11600-5

[10] Liu H, Qian S and Bau H H 2007 The effect of translocating cylindrical particles on the ionic current through a nanopore *Biophys. J.* **92** 1164-77

[11] Gigliotti B, Sakizzie B, Bethune D S, Shelby R M and Cha J N 2006 Sequence-independent helical wrapping of single-walled carbon nanotubes by long genomic DNA *Nano Lett.* **6** 159-64

[12] Rajendra J, Baxendale M, Dit Rap L G and Rodger A 2004 Flow linear dichroism to probe binding of aromatic molecules and DNA to single-walled carbon nanotubes *J. Am. Chem. Soc.* **126** 11182-8

[13] Dukovic G, Balaz M, Doak P, Berova N D, Zheng M, McLean R S and Brus L E 2006 Racemic single-walled carbon nanotubes exhibit circular dichroism when wrapped with DNA *J. Am. Chem. Soc.* **128** 9004-5

[14] Heller D A, Jeng E S, Yeung T-K, Martinez B M, Moll A E, Gastala J B and Strano M S 2006 Optical detection of DNA conformational polymorphism on single-walled carbon nanotubes *Science* **311** 508-11

[15] Star C, Tu E, Niemann J, Gariel J-C P, Joiner C S and Valcke C 2006 Label-free detection of DNA hybridization using carbon nanotube network field-effect transistors *Proc. Nat. Acad. Sci. U.S.A.* **103** 921-6

[16] Yang Q-H, Gale N, Oton C J, Li F, Vaughan A, Saito R, Nandhakumar I S, Tang Z-Y, Cheng H-M, Brown T and Loh W H 2007 Raman probe for selective wrapping of single-walled carbon nanotubes by DNA *Nanotechnology* **18** 405706-1 - -5

[17] Huang X, McLean R S and Zheng M 2005 High-resolution length sorting and purification of DNA-wrapped carbon nanotubes *Anal. Chem.* **77** 6225-8
[18] Gao H and Kong Y 2004 Simulation of DNA-nanotube interactions *Ann. Review Matt. Research* **34** 123-50
[19] Manohar S, Tang T and Jagota A 2007 Structure of homopolymer DNA - CNT hybrids *J. Phys. Chem. C* **111** 17835-45
[20] Tu X, Manohar S, Jagota A and Zheng M 2009 DNA sequence motifs for structure-specific recognition and separation of carbon nanotubes *Nature* **460** 250-3
[21] Huang X M H, Caldwell R, Huang L, Jun S C, Huang M, Sfeir M Y, O'Brien S P and Hone J 2005 Controlled placement of individual carbon nanotubes *Nano Lett.* **5** 1515-8
[22] Arnold M S, Green A A, Hulvat J F, Stupp S I and Hersam M C 2006 Sorting carbon nanotubes by electronic structure using density differentiation *Nature Nanotechnology* **1** 60-5
[23] LeMieux M C, Roberts M, Barman S, Jin Y W, Kim J M and Bao Z 2008 Self-sorted, aligned nanotube networks for thin-film transistors *Science* **321** 101-4
[24] Lin T, Taylor S, Li H, Fernando K A S, Qu L, Wang W, Gu L, Zhou B and Sun Y-P 2004 Advances toward bioapplications of carbon nanotubes *J. Mater. Chem.* **14** 527-41
[25] 2005 *Carbon Nanotechnologies Inc. Product Description, HiPco Single-Walled Carbon Nanotubes* (Houston, TX: Carbon Nanotechnologies Inc.)
[26] Vogel S R, Kappes M M, Hennrich F and Richert C 2007 An unexpected new optimum in the structure space of DNA solubilizing single-walled carbon nanotubes *Chem. Eur. J.* **13** 1815-20
[27] Niyogi S, Hamon M A, Perea D E, Kang C B, Zhao B, Pal S K, Wyant A E, Itkis M E and Haddon R C 2003 Ultrasonic dispersions of single-walled carbon nanotubes *J. Phys. Chem. B* **107** 8799-804
[28] Jeng E S, Moll A E, Roy A C, Gastala J B and Strano M S 2006 Detection of DNA hybridization using the near-infrared band-gap fluorescence of single-walled carbon nanotubes *Nano Lett.* **6** 371-5
[29] Jeng E S, Barone P W, Nelson J D and Strano M S 2007 Hibridization kinetics and thermodynamics of DNA adsorbed to individually dispersed single-walled carbon nanotubes *Small* **3** 1602
[30] Bates R G 1962 Revised standard values for pH measurements from 0 to 95 C *J. Res. Natn. Bur. Stand.* **66A** 179
[31] Huang H, Kajiura H, Maruyama R, Kadono K and Noda K 2006 Relative optical absorption of metallic and semiconducting single-walled carbon nanotubes *J. Phys. Chem. B* **110** 4686-90
[32] Sambrook J, Fritsch E F and Maniatis T 1989 *Molecular Cloning. A Laboratory Manual.* (Cold Spring Harbor, NY: Cold Spring Harbor Laboratory Press)
[33] Chen R J and Zhang Y 2006 Controlled precipitation of solubilized carbon nanotubes by delamination of DNA *J. Phys. Chem. B.* **110** 54-7
[34] Johnson R R, Johnson A T C and Klein M L 2008 Probing the structure of DNA-carbon nanotube hybrids with molecular dynamics *Nano Lett.* **8** 69-75
[35] Martin W, Zhu W and Krilov G 2008 Simulation study of noncovalent hybridization of carbon nanotubes by single-stranded DNA in water *J. Phys. Chem. B* **112** 16076-89
[36] Phillips K, Dauter Z, Murchie A I H, Lilley D M J and Luisi B 1997 The crystal strucutre of parallel-stranded guanine tetraplex at 0.95A resolution *J. Mol. Biol.* **273** 171-82
[37] Voet D, Gratzer W B, Cox R A and Doty P 1963 Absorption spectra of nucleotides, polynucleotides, and nucleic acids in the far ultraviolet *Biopolymers* **1** 193-208

[38] Tinoco I 1960 Hypochroism in polynucleotides *J. Am. Chem. Soc.* **82** 4785-90
[39] Sowers L C, Shaw B R and Sedwick W D 1987 Base stacking and molecular polarizability: Effect of a methyl group in the 5-position of pyrimidines *Nucleic Acids Res.* **148** 790-4
[40] Ghosh A and Bansal M 2003 A glossary of DNA structures from A to Z *Acta Crystallographica Section D* **D59** 620-6
[41] Bloomfield V A, Crothers D M and Tinoco I J eds 1999 *Nucleic Acids - Structures, Properties, and Functions* (Sausalito, CA: University Science Books)
[42] Lustig S R, Jagota A, Khripin C and Zheng M 2005 Theory of structure-based carbon nanotube separations by ion-exchange chromatography of DNA/CNT hybrids *J. Phys. Chem. B* **109** 2559-66
[43] Gardiner W C 1969 *Rates and Mechanisms of Chemical Reactions.* (New York: W.A. Benjamin, Inc.)
[44] Cathcart H, Nicolosi V, Hughes J M, Blau W J, Kelly J M, Quinn S J and Coleman J N 2008 Ordered DNA wrapping switches on luminescence in single-walled nanotube dispersions *J. Amer. Chem. Soc.* **130** 12734-44
[45] Keleti T 1983 Error in the evaluation of Arrhenius and van't Hoff Plots *Biochem J.* **209** 277-80
[46] Johnson R R, Kohlmeyer A, Johnson A T C and Klein M L 2009 Free energy landscape of a DNA-carbon nanotube hybrid using replica exchange molecular dynamics *Nano Lett.* **9** 537-41
[47] Manohar S, Mantz A R, Bancroft K E, Hui C-Y, Jagota A and Vezenov D V 2008 Peeling single-stranded DNA from graphite surface to determine oligonucleotide binding energy by force spectroscopy *Nano Lett.* **8** 4365-72
[48] Sowerby S J, Cohn C A, Heckl W M and Holm N G 2001 Differential adsorption of nucleic acid bases: Relevance to the origin of life *Proc. Natl. Acad. Sci.* **98** 820-2
[49] Guckian K M, Schweitzer B A, Ren R X, Sheils C J, Tahmassebi D C and Kool E T 2000 Factors contributing to aromatic stacking in water: Evaluation in the context of DNA *J. Am. Chem. Soc.* **122** 2213-22

FIGURE CAPTIONS

Figure 1. Cartoon representation of experimental schemes (not to scale). Dissociation of DNA from dispersed DNA/SWNT leads to aggregation of the nanotubes. The aggregates were removed by centrifugation and the dissociation process was monitored by determining the fraction of the initially purified DNA/SWNT dispersion that remained suspended after the preparation had been incubated (1) at different temperatures for 10.0 min, or (2) at room temperature after addition of different concentrations of free DNA, or (3) at a desired temperature for different lengths of time.

Figure 2. Nucleobase dependence of DNA/SWNT dissociation. The fraction of total initial DNA/SWNT that remained suspended after 10 min. was plotted as a function of temperature for poly $d(G)_{12}$, $d(C)_{12}$, $d(T)_{12}$, and $d(A)_{12}$ and fitted to the sigmoidal function $y = y_o + a/1 + e$, where T is the temperature in degrees C and a, b and y_o are parameters of the fit. (Inset) Results of an independent experiment with nanotubes associated with dT_{12} DNA in which the measured concentration of free DNA unbound from the $d(T)_{12}$/SWNTs after 10 min. as a function of temperature was superimposed on the plot showing the fraction of $d(T)_{12}$/SWNT that remained suspended.

Figure 3. Effect of alternating bases on DNA/SWNT stability. The fraction of total initial DNA/SWNT that remained suspended after 10 min. was plotted as a function of temperature for poly $d(AC)_6$/SWNT and $d(GT)_6$/SWNT.

Figure 4. Dissociation kinetics of d(T12)/SWNT at room temperature. (a) The solid line is a fit to an exponential decay with a fractional offset d = 0.22 (see equation 2) and a $T_{1/2}$ for the first order process = 41 h. (b) The fraction of total initial dispersed $d(T)_{12}$/SWNT that remained suspended after 480 hours at room temperature as a function of free DNA added at t = 0 h.

Figure 5. Tuning the thermal dissociation of DNA/SWNTs. Upon addition of 140μM free poly $d(T)_{12}$ ssDNA to a $d(T)_{12}$/SWNT dispersion, the hybrid dissociation temperature ($T_{½}$), measured by the isochronal temperature assay, was shifted to a higher temperature.

Figure 6. Temperature dependence of the rate of hybrid dissociation. (a) The fraction of total initial $d(A)_{12}$/SWNT that remained suspended plotted as a function of time at four different temperatures. (b) Eyring plots of similar data for nanotubes associated with poly $d(A)_{12}$, $d(C)_{12}$, and $d(T)_{12}$. The slopes of the lines reveal the activation enthalpy of DNA unbinding from nanotubes (Table 1) and show the same nucleobase trend as observed in the isochronal temperature plots of figure 2.

Table 1. DNA/SWNT hybrid dissociation thermodynamic and kinetic parameters. The dissociation temperatures, activation enthalpies, and rate constants were determined from isochronal dissociation assays, Eyring analysis, and dissociation kinetics, respectively.

	Dissociation Temperature	**Activation Enthalpy**	**Dissociation rate at 99°C**	
Oligo	**$T_{1/2}$ (°C)**	**ΔH (kcal/mole)**	**k_{off}(min^{-1})[a]**	**τ (min)[a]**
$d(G)_{12}$	> 100.0[b]	N.D.	<0.005[b]	>135[b]
$d(C)_{12}$	96.0 ± 2.6	24.4 ± 0.2	0.13± 0.02	5.3± 0.3
$d(A)_{12}$	74.0 ± 3.0	20.3 ± 1.6	0.58± 0.01	1.2± 0.2
$d(T)_{12}$	71.0 ± 1.0	14.8 ± 1.1	1.03± 0.04	0.7± 0.2
$d(GT)_6$	85.0 ± 9.1	N.D.	N.D.	N.D.
$d(AC)_6$	61.0 ± 7.1	N.D.	N.D.	N.D.

[a] Dissociation rate constant k_{off} is obtained from the fit to an exponential decay (Eq. 2) for the first order process. The value of τ is the time at which 50% of the hybrids remain in solution.

[b] Because poly $d(G)_{12}$ exhibits slow dissociation rates at 99°C (exceeding the assay time), the values of k and τ are estimates from the fits to Eq. 2.

Figure 1

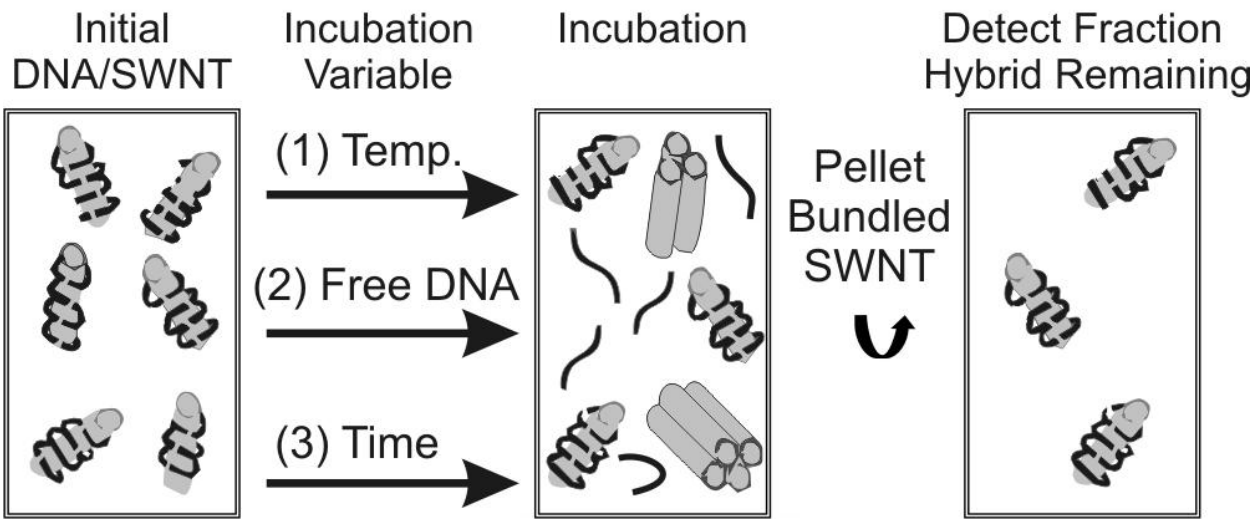
Initial
DNA/SWNT
Incubation
Variable
(1) Temp.
(2) Free DNA
(3) Time
Incubation
Pellet
Bundled
SWNT
Detect Fraction
Hybrid Remaining

Figure 2

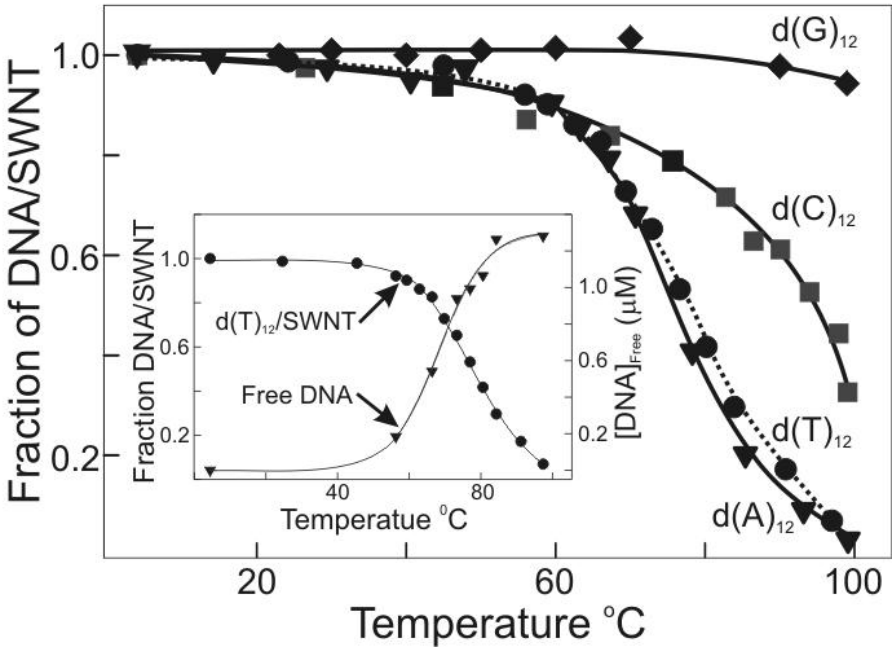
Fraction of DNA/SWNT
1.0
0.6
0.2
20
60
100
Temperature °C
d(G)12
d(C)12
d(T)12
d(A)12
Fraction DNA/SWNT
d(T)12/SWNT
Free DNA
[DNA]Free (μM)
40
80
Temperatue °C

Figure 3

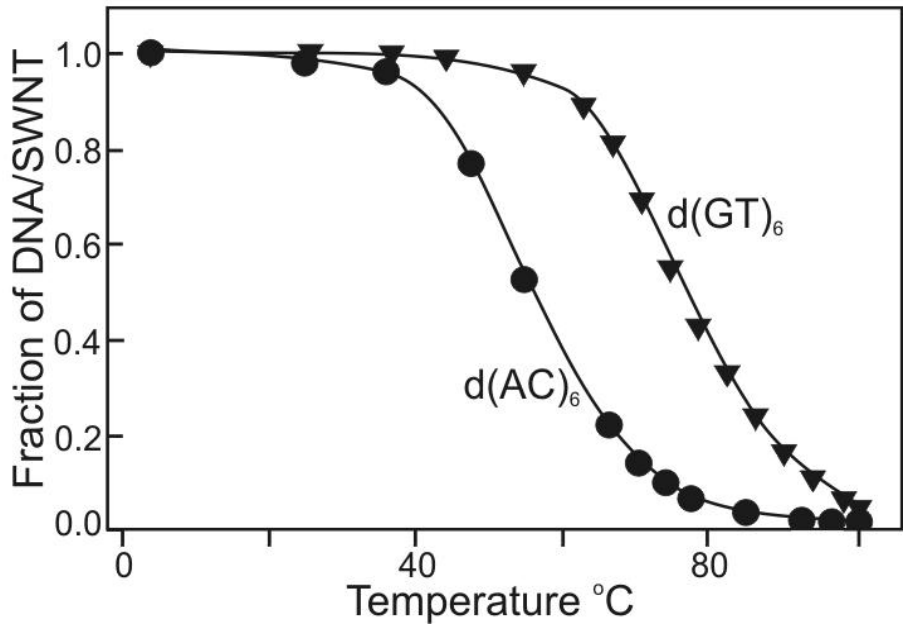

Figure 4

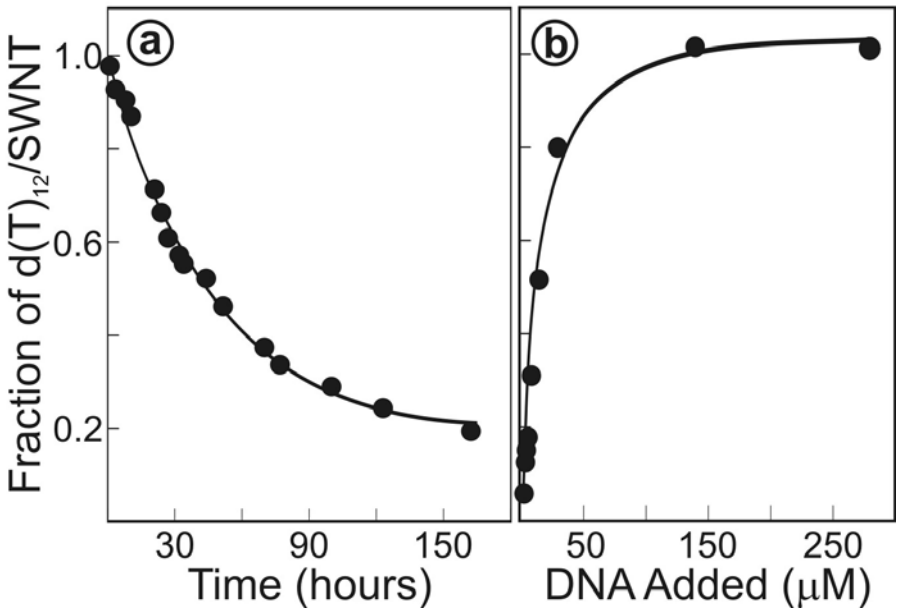

Figure 5

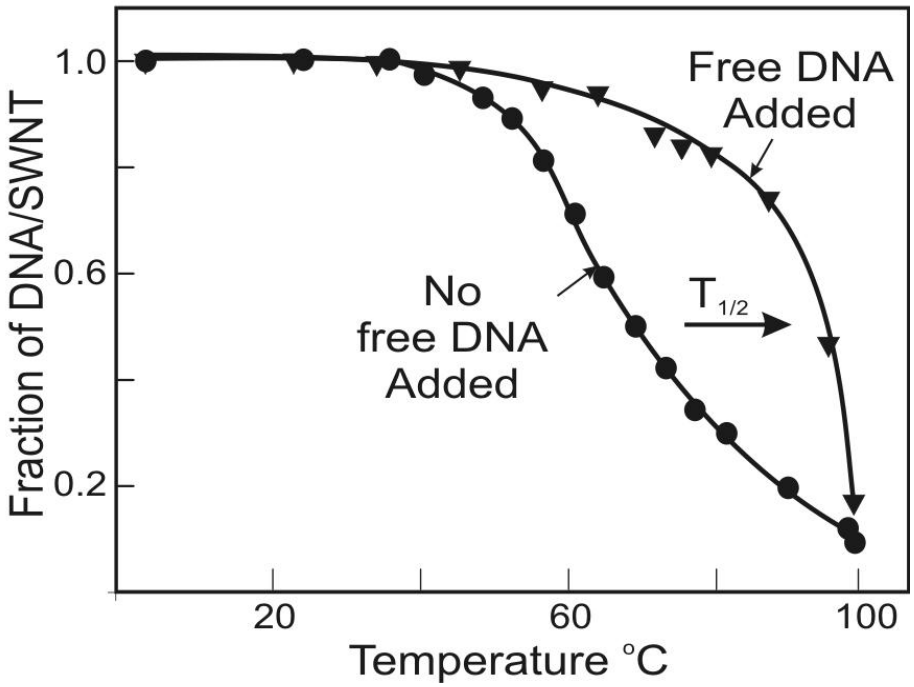
1.0
0.6
0.2
Fraction of DNA/SWNT
Free DNA
Added
No
free DNA
Added
T1/2
20
60
100
Temperature °C

Figure 6

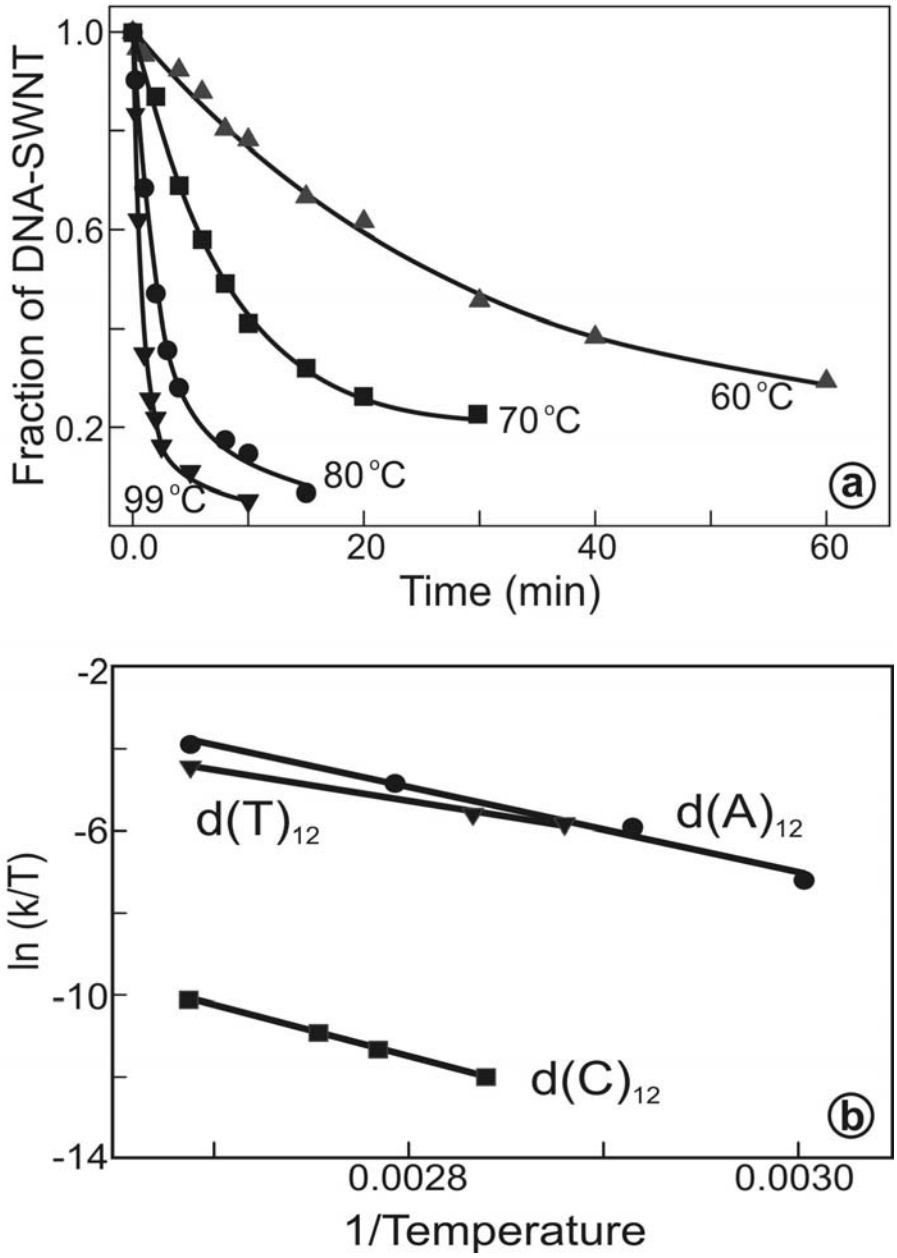
1.0
0.6
0.2
Fraction of DNA-SWNT
60°C
70°C
80°C
99°C
a
0.0
20
40
60
Time (min)
-2
-6
-10
-14
ln (k/T)
d(T)12
d(A)12
d(C)12
b
0.0028
0.0030
1/Temperature